Lipid droplet storage promotes murine pancreatic tumor growth

JEREMY J. GRACHAN[1], MARTIN KERY[1], AMATO J. GIACCIA[2], NICHOLAS C. DENKO[1] and IOANNA PAPANDREOU[1,3]

[1]Department of Radiation Oncology, The Ohio State University Comprehensive Cancer Center, Columbus, OH 43210; [2]Department of Radiation Oncology, Stanford University, Stanford, CA 94305; [3]Department of Radiation Oncology, The Ohio State University Comprehensive Cancer Center, Columbus, OH 43210, USA

Received August 14, 2020; Accepted November 20, 2020

DOI: 10.3892/or.2021.7972

Abstract. Hypoxia Inducible Lipid Droplet Associated (HILPDA) is frequently overexpressed in tumors and promotes neutral lipid storage. The impact of Hilpda on pancreatic ductal adenocarcinoma (PDAC) tumor growth is not known. In order to evaluate Hilpda-dependent lipid storage mechanisms, expression of Hilpda in murine pancreatic cells (KPC) was genetically manipulated. Lipid droplet (LD) abundance and triglyceride content *in vitro* were measured, and model tumor growth in nu/nu mice was determined. The results showed that excess lipid supply increased triglyceride storage and LD formation in KPC cells in a HILPDA-dependent manner. Contrary to published results, inhibition of Adipose Triglyceride Lipase (ATGL) did not ameliorate the triglyceride abundance differences between Hilpda WT and KO cells. Hilpda ablation significantly decreased the growth rate of model tumors in immunocompromised mice. In conclusion, Hilpda is a positive regulator of triglyceride storage and lipid droplet formation in murine pancreatic cancer cells *in vitro* and lipid accumulation and tumor growth *in vivo*. Our data suggest that deregulated ATGL is not responsible for the absence of LDs in KO cells in this context.

Introduction

Metabolic changes have been recognized as one of the hallmarks of cancer (1). These changes, which can be genetically determined by specific oncogenic alterations and be impacted by tumor microenvironmental conditions, serve multiple adaptive roles that are incompletely understood. Among them are the growing tumors' high anabolic demands, and the defense from pathological conditions created by this uncontrolled growth.

Correspondence to: Dr Ioanna Papandreou, Department of Radiation Oncology, The Ohio State University Comprehensive Cancer Center, 420 W. 12th Avenue, Columbus, OH 43210, USA
E-mail: ioanna.papandreou@osumc.edu

Key words: lipid, hypoxia, pancreatic

Pancreatic cancer is often hypoxic with a poor 8% survival rate at 5 years (2), and is immunologically privileged (3).

Mutated KRAS is the most commonly found oncogenic event in pancreatic ductal adenocarcinoma (PDAC) and is responsible for the initiation of tumor metabolic reprograming (4,5). Similarly to other Ras-driven cancers, the metabolic needs of PDAC have been shown to depend on scavenging of extracellular nutrient sources (6). These nutrients, such as proteins, nucleotides and lipids enter cells through macropinocytosis, a well-described KRAS-dependent mechanism of membrane budding and subsequent cargo vesicle trafficking (6-8). Fatty acid (FA) synthesis in PDAC may be attenuated and intracellular pool of FAs derived predominantly from exogenous sources, such as serum lysophospholipids (9-12). Accordingly, cholesterol uptake in PDAC has been shown to be indispensable for sustaining proliferative capacity of PDAC. Silencing of low-density lipoprotein receptor (LDLR) that translocates cholesterol-rich LDLs sensitizes PDAC to chemotherapy (13). Glucose and glutamine metabolism are also regulated by oncogenic Kras, which can change the source of acetyl-CoA production that is being used for fatty acid synthesis (14).

Part of the metabolic rewiring involves the increased storage of neutral lipids inside lipid droplets (LDs). The core of LDs contains esterified fatty acids and cholesterol species and is separated from the hydrophilic cytosol by a phospholipid monolayer. On the periphery, associated proteins control the access of enzymes in a regulated manner and determine the dynamics of LD turnover (15).

HILPDA is a small, evolutionarily young protein that was originally identified through its induction by oxygen- or glucose deprivation (16). It localizes to LDs and the endoplasmic reticulum and promotes lipid storage in a large number of cell types tested, including cancer cells, hepatocytes, and macrophages (17-20). Whole body ablation of Hilpda in mice results in a thermoregulatory defect in fasted mice, suggesting a systemic role in fuel utilization (21). Various cell type-specific genetic models have identified defects in lipid turnover by Hilpda loss, however, the precise molecular target of Hilpda's action remained elusive (18,19,22,23). Recently, it was demonstrated that Hilpda can promote LD formation by binding and inhibiting Adipose Triglyceride Lipase (ATGL/PNPLA2), which is the first and rate-limiting enzyme in triglyceride hydrolysis (24,25). Furthermore, we identified HILPDA-dependent inhibition of ATGL during states of high

lipid turnover such as fatty acid supplementation or starvation-induced LD remodeling (26). This molecular mechanism controlling triglyceride accumulation was important for colon and lung model tumor growth (24,26).

The aim of the present study was to determine whether Hilpda-dependent regulation of lipid metabolism plays a role in the *in vivo* growth of model murine pancreatic tumors and which biochemical perturbations are caused by Hilpda deletion.

Materials and methods

Cell culture and treatments. KPC cells were originally established from the Tuveson LSL-Kras G12D/+; LSL-Trp53R172H/+; Pdx-1-Cre model (27) and were grown in DMEM + 10% FBS (Gibco) in a humidified incubator at 37˚C. ATGListatin (20 μM), drug vehicle control DMSO, docosahexanoic acid (DHA) (60.7 μM) (all from Sigma-Aldrich; Merck KGaA) were used as indicated for various experiments. Western blots were repeated twice, biochemical assays were performed in four independent biological replicates. All treatments were performed at 37˚C.

Molecular cloning and transfections. HILPDA KO cell lines were generated using a double nickase strategy. Two gRNAs targeting Hilpda: A (5'-TCTAACAAAGATGGAAAGCA-3') and B (5'-GGAGTCTCTGGGAGGCTTAC-3') were individually cloned in pX462-Cas9n backbone [pSpCas9n(BB)-2A-Puro V2.0, Addgene: 62987] using *Bbs*I restriction site. Constructs targeting Hilpda were sequence-verified and used to create Hilpda KO cell lines. Cells were transfected with 2 μg DNA using Lipofectamine 2000 (Thermo Fisher Scientific). Single clones were selected by antibiotic resistance for 3 days and further expansion for 2 weeks, screened by westerns blotting and 7 successful KO clones were combined to generate the KO pool. The pIRES-neo-Hilpda-myc-flag expression vector has been described previously (26). Cells were transfected with pIRES-neo-Hilpda-myc-flag or empty vector pIRES-neo (Origene) and underwent G418 (Sigma-Aldrich; Merck KGaA) selection at 2 mg/ml for 2 weeks before being screened for transgene expression.

Western blot analysis. KPC cells were lysed in RIPA buffer (150 mM NaCl, 1% NP 40, 0.5% sodium deoxycholate, 0.1% SDS, 50 mM Tris, pH 8.0) supplemented with 100X Halt protease inhibitor cocktail (Thermo Scientific Fisher), 100X phosphatase inhibitor cocktail (Cell Signaling Technology) and 1 mM PMSF (Thermo Fisher Scientific). Lysates were cleared by centrifugation for 5 min at 12,000 x g and at 4˚C. Protein concentrations were measured with a bicinchoninic acid (BCA) protein kit (Thermo Scientific Fisher). Then, 20-30 μg of whole protein lysates were resolved in an 11% acrylamide gel and transferred onto PVDF membrane. For immunodetection, primary antibodies used were: Custom-made rabbit anti-Hilpda 1:50 (21), rabbit a-Perilipin2 (1:1,000; Origene, cat. no. TA321279), mouse a-myc (1:1,000; Cell Signaling Technology, cat. no. 2276S), and rabbit a-ATGL (1:1,000; Cell Signaling Technology, cat. no. 2138S), and mouse a-tubulin (1:1,000; Invitrogen; Thermo Fisher Scientific, cat. no. PIMA516308). Primary antibodies were detected using Licor goat anti-mouse (1:2,000, Licor, cat. no. 926-68070) or goat anti-rabbit (1:2,000; Licor, cat. no. 926-32211) secondary antibodies, and visualized using a Licor Odyssey CLx near infrared imager.

Fluorescence microscopy. Cells were grown on glass coverslips, treated as required and fixed with 4% paraformaldehyde. Lipid droplets were stained with 0.1 μg/ml Nile Red (Santa Cruz Biotechnology) for 20 min at room temperature. Nuclei were counterstained with 10 μg/ml Hoechst-33342, and samples were mounted with Slowfade Diamond antifade mounting media (Life Technologies, cat. no. S36968). The slides were imaged on a Zeiss Axioskope widefield microscope at the OSUCCC microscopy and imaging facility. Lipid droplet images were visualized with ImageJ.

Triglyceride quantification. Cells were grown on 10 cm culture dishes in regular DMEM media, and fatty acid was loaded (using DHA), or starved of FBS for 24 h. Where indicated, ATGListatin was added at the beginning of treatment. Triglycerides were measured using the colorimentric Triglyceride Quantification Assay Kit (Abcam; cat. no. ab65336) as per the manufacturer's recommendation (sensitivity >2 μM).

In vivo xenograft growth. All animal experiments were approved by the Ohio State University's Institutional Animal Care and Use Committee. Five hundred thousand cells in PBS were injected subcutaneously on the back of non-anesthetized 7- to 9-week-old female nu/nu mice (18-21 g) obtained from the OSUCCC Target Validation Shared Resource (n=11/group). Groups of 3-4 animals were housed in autoclaved cages, were fed *ad libitum*, and maintained on a 12-h light/dark cycle. Room temperature was maintained at 22˚C and humidity at 30%. Cages were randomly assigned to experimental groups. Tumor growth was measured using calipers. Tumor volume was calculated using the formula: S x S x W x 0.52. Animals were euthanized by CO_2 asphyxiation followed by cervical dislocation according to the approved protocol. Maximal tumor dimensions at the time of sacrifice were 12 and 8 mm in the WT and KO groups, respectively.

Statistical analysis. Using SPSS v25, data were screened for normality and homogeneity of variance using the Shapiro-Wilk and Levene tests, respectively. When normality and equal variance was met, a Student's t-test was used. When normality and equal variance was not met, a non-parametric Mann-Whitney U test was used. Data were considered to be statistically significant if $P<0.05$. Kaplan-Meier curves were compared by the Xena Browser using the log-rank test (www.xenabrowser.net).

Results

Microenvironmental stresses regulate Hilpda levels in KPC cells. We and others have shown that conditions that increase lipid flux can induce Hilpda protein (17,24,26). To determine whether similar mechanisms exist in murine pancreatic tumor cells, we exposed KPC cells to regular normoxic conditions in DMEM media, to oxygen deprivation (1% O_2) or to exogenous

fatty acid (docosahexaenoic acid) for 24 h and examined Hilpda protein expression by western blot analysis (Fig. 1A). As has been reported in other tumor types, both hypoxia and fatty acid loading increased Hilpda levels in KPC cells. Expression of ATGL was detectable under all conditions but was not stress-responsive. To evaluate the possible impact of HILPDA expression in the clinical behavior of human pancreatic cancers we assessed the TCGA PDAC dataset using the Xena functional genomics explorer (xenabrowser.net). PDAC tumors with the highest quartile HILPDA expression had a significantly shorter overall survival than those with the lowest expression (Fig. 1B), suggesting that HILPDA may be associated with more aggressive cancers.

Hilpda promotes LD abundance. We genetically manipulated Hilpda in KPC cells and asked whether it is necessary or sufficient for LD growth *in vitro* under different growth conditions. The impact of Hilpda on the ability of cells to form lipid droplets appears to be cell-type specific. First, Hilpda KO cells were generated by CRISPR-Cas9 gene editing and single clones were screened for successful gene deletion (data not shown). A pool of 7 KO clones was established and loss of Hilpda protein expression was confirmed (Fig. 2A). In parallel, a KPC cell line stably overexpressing myc-Flag tagged Hilpda driven by the CMV promoter was generated (Fig. 2B). Next, we determined whether the engineered cells have perturbations in LD dynamics. Cells were incubated in different nutritional states that are known to increase lipid flux: Exogenous fatty acid supplementation and lipid deprivation through serum removal. After 24 h, cells were fixed with 4% paraformaldehyde and lipid droplets were visualized by fluorescence microscopy after staining with the neutral lipid dye Nile Red. Hilpda overexpression led to an increase in LD abundance compared to empty vector cells, under all conditions. Conversely, under all environmental conditions, the *Hilpda* KO cells had smaller and fewer lipid droplets, suggesting that Hilpda positively regulates lipid droplet abundance.

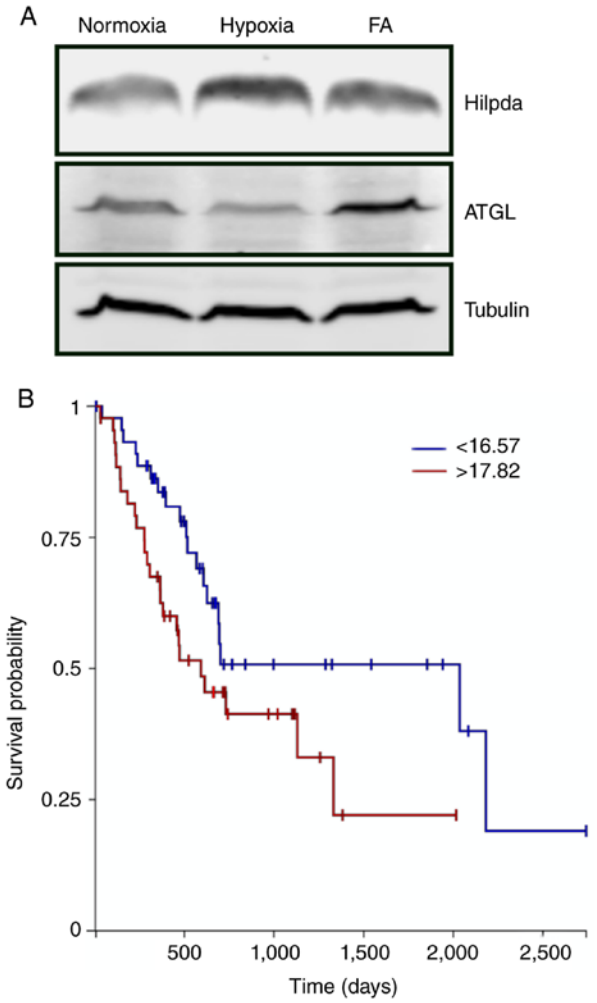

Figure 1. Hilpda is stress-inducible in KPC. (A) Cells were maintained in complete media at 21% O_2 (normoxia), placed in 1% O_2 (hypoxia) or supplemented with 60.7 μM DHA (FA) for 24 h. Protein expression was determined by western blotting. (B) Overall survival of the TCGA pancreatic cancer (PAAD) dataset according to HILPDA expression. Top quartile: n=44, bottom quartile: n=46. P=0.049.

Hilpda promotes triglyceride storage in KPC cells, independently of ATGL inhibition. Qualitative and quantitative differences in the constitution of LD's neutral lipid core have been identified (28). To ascertain whether the differences in LD abundance caused by Hilpda loss in KPC results from deregulated triglyceride metabolism, we biochemically quantified triglyceride levels under basal- and fatty acid-loaded conditions (Fig. 3A). In accordance with the LD staining results, the Hilpda KO cells were significantly impaired in their maximum triglyceride storage capacity. In basal conditions there was a trend towards lower triglycerides in the KOs but did not reach statistical significance.

We and others have shown that in certain tissue contexts Hilpda promotes triglyceride storage by inhibiting the rate-limiting lipase ATGL/PNPLA2 (24-26). In order to establish if Hilpda functions as a molecular ATGL inhibitor in murine pancreatic tumors, we pharmacologically inhibited ATGL in Hilpda WT and KO cells with the small molecule inhibitor ATGListatin (ATGLi), and quantified triglycerides (Fig. 3B). Notably, the chemical inhibition of ATGL was not able to correct the defect in the KOs and to restore their triglyceride content to the level of the Hilpda WT cells. This finding suggests that, in KPC cells, decreased lipid storage following Hilpda ablation is not caused by elevated ATGL activity and enhanced lipolysis.

Hilpda promotes model tumor growth. Loss of Hilpda-dependent ATGL regulation has been shown to be growth inhibitory in model tumors (24,26). Owing to the *in vitro* findings of ATGL-independent Hilpda functions in KPC we examined whether Hilpda exerts tumor-promoting properties in pancreatic cancer xenografts. WT and KO cells were injected subcutaneously into the backs of nude mice (11 mice per genotype) and tumor sizes were measured with calipers. The results showed that loss of Hilpda significantly decreased the growth rate of KPC tumors, suggesting that Hilpda can positively regulate tumor growth, independently of lipolytic control (Fig. 4A and B). At the completion of the xenograft growth, we excised the tumors and confirmed their Hilpda genotype by western blot analysis (Fig. 4C) and measured their triglyceride content (P<0.05) (Fig. 4D). The WT tumors contained two times more triglycerides than the KOs, indicating that tumor microenvironmental conditions, such as hypoxia, stimulate Hilpda-dependent lipid storage.

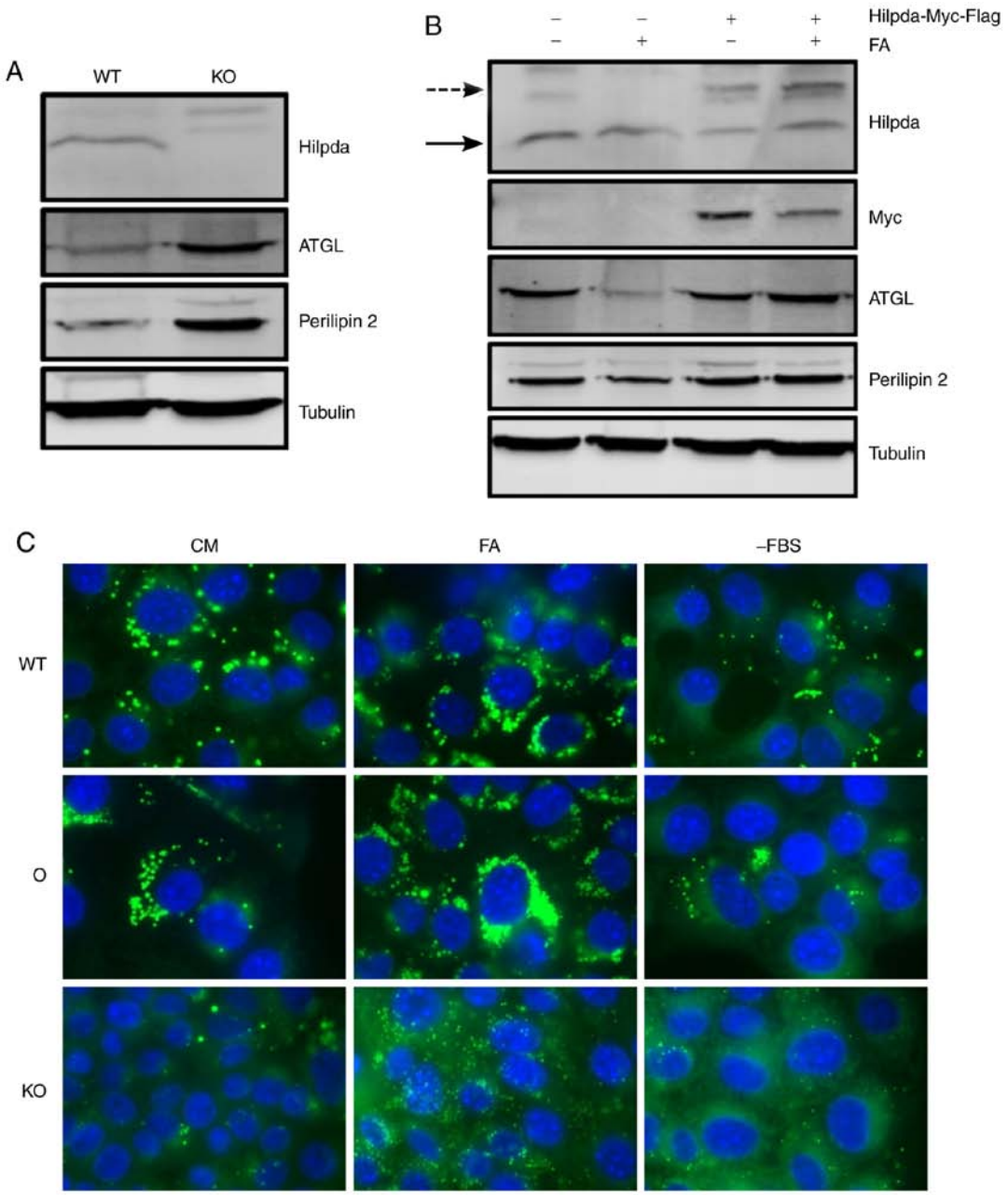

Figure 2. Hilpda regulates LD abundance in KPC. (A) KO cells were generated by CRISPR-Cas9 gene editing followed by neomycin resistance selection. Seven individual KO clones were pooled and Hilpda status in media containing 60.7 μM DHA was verified by western blotting. (B) Establishment of Hilpda overexpressing cells. KPC were transfected with a pIRESneo-Hilpda-myc-Flag plasmid and selected by neomycin resistance. Expression of endogenous and exogenous Hilpda was confirmed in a pool of antibiotic-resistant cells prior- and after-supplementation with 60.7 μM DHA (solid arrow: Endogenous Hilpda, broken arrow: Hilpda-myc-Flag). (C) Hilpda controls neutral lipid storage. Fluorescent microscopy of LDs in genetically manipulated KPC cells under different nutritional variations. Wild-type KPC (WT), *Hilpda* overexpressor (O), and neomycin-resistant knockout cells (KO) were grown in complete media (CM), supplemented with 60.7 μM DHA (FA) or deprived of lipids in FBS-free media for 24 h. Fixed cells were stained with Nile Red to detect lipids (green) and nuclei counterstained with Hoechst-33342. Hilpda expression was associated with abundance of detectable LDs. Representative images from one of two independent experiments are shown.

Discussion

Rewiring of lipid flux pathways is a common feature of malignancies and has important biological and clinical implications. In the context of Ras-driven cancers, inhibition of Fatty Acid Synthase (FASN) impaired growth, suggesting an active pathway of *de novo* fatty acid synthesis (29,30). Other reports have shown an increase in exogenous lipid uptake, storage, and utilization, as mechanisms that support cell growth and malignant progression (9,31). Although the source of lipids may depend on many genetic and experimental factors, hypoxia and nutrient availability in the tumor microenvironment can shift the balance towards storage of esterified lipids (32), in part through the upregulation of LD-associated proteins.

A key question surrounding the pro-tumorigenic effects of LDs is how they can protect from cell death or promote proliferation. Several biological mechanisms that mitigate, through LD dynamics, nutrient fluctuations in the tumor microenvironment have been identified. These include

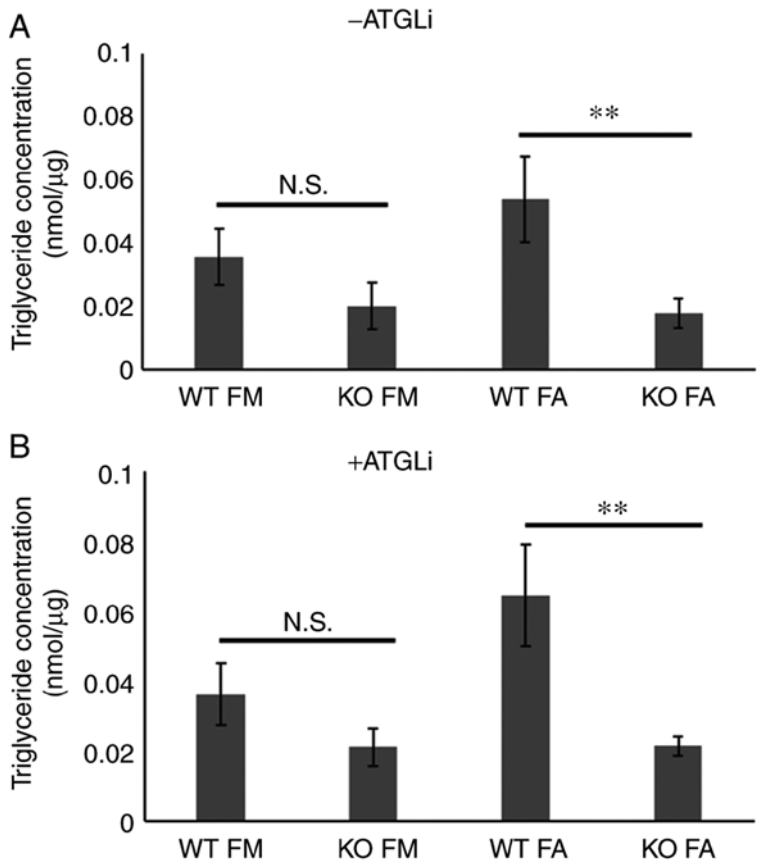

Figure 3. Quantification of triglycerides in *Hilpda*-manipulated KPC cells. Wild-type and *Hilpda* knockout KPC cells were kept under basal (full media, FM) or fatty acid loaded (FA) conditions for 24 h. Triglyceride levels for wild-type (WT) and neomycin *Hilpda* knockout cells (KO), without (A) or with (B) ATGListatin treatment (Ai, 20 μM) were measured by a biochemical assay. Hilpda loss decreased the capacity to store triglycerides independently of ATGL activity. (n=4, **P<0.01, N.S. not significant by Student's t-test and Mann Whitney U test).

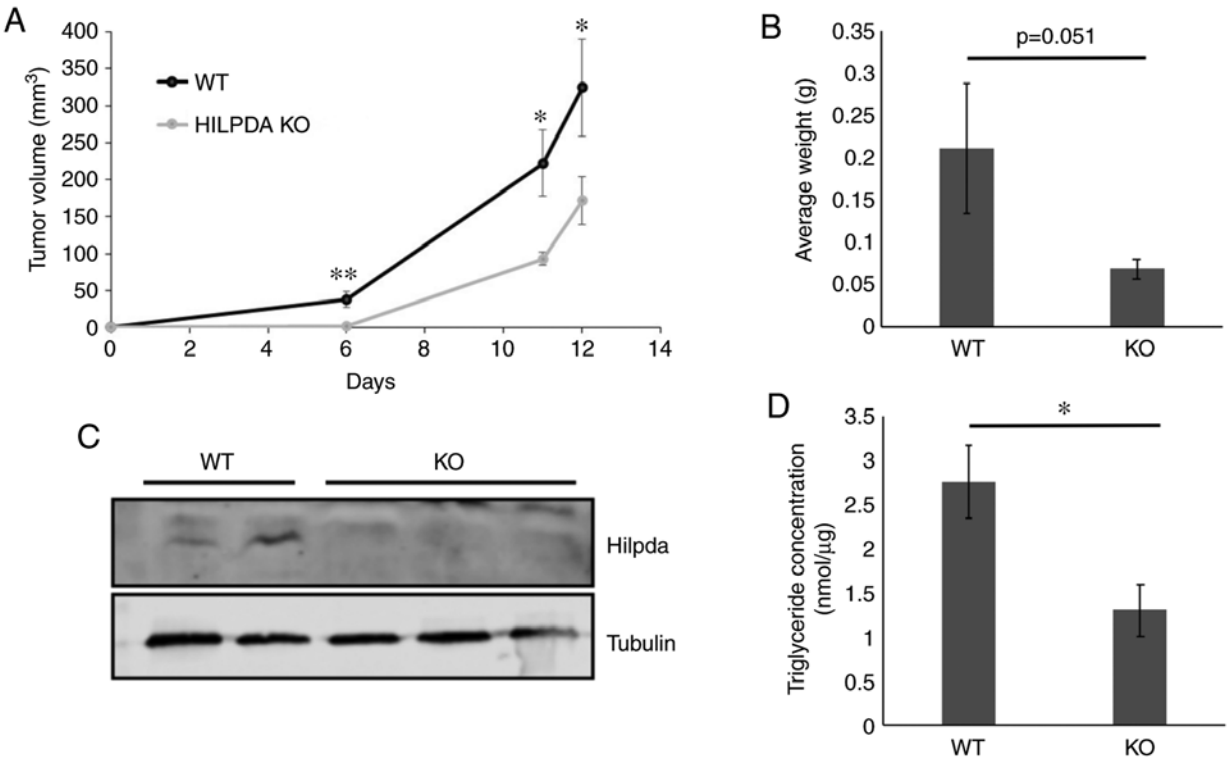

Figure 4. Hilpda promotes tumor growth. (A) *In vivo* growth of subcutaneous KPC model tumors in nude mice was monitored by caliper measurements (n=11). (B) Final tumor weight of excised tumors. (C) Hilpda protein expression in tumor extracts (D) Triglyceride quantification in tumor extracts (n=3). Hilpda KO tumors grew more slowly, maintained their KO status and contained lower amounts of stored lipids. (*P<0.05, **P<0.01, by Student's t-test and Mann Whitney U test).

protection from oxidative stress during reoxygenation after hypoxia (33), from membrane disruption and ER stress (34,35), protection of mitochondrial integrity and function during starvation (36-38), and sequestration of death-inducing fatty acid metabolites (39,40).

In particular, HILPDA expression is regulated by both hypoxia and fatty acid supplementation (41). In turn, that determines the biochemical composition of LD content and promotes tumor growth *in vivo*. In the present study, we confirmed that Hilpda expression is induced by hypoxia in murine pancreatic cells, as has been shown for other anatomical sites (17,24,26). In agreement with previous studies conducted by us and others on other model systems, HILPDA ablation significantly decreased triglyceride content and retarded KPC xenograft tumor growth (24,26,42). Previously, we have shown that uncontrolled ATGL activity is responsible for triglyceride loss after Hilpda ablation in MEFs and colorectal cancer models (26); however, our data suggest that in pancreatic cancer Hilpda's major biological mechanism does not involve inhibition of ATGL-initiated lipolysis. This explanation is based on the inability of a specific ATGL inhibitor to restore LD abundance in the HILPDA-deficient cells. Interestingly, a recent preprint provides evidence for a novel function of Hilpda as a positive regulator of triglyceride synthesis, via the stimulation of DGAT1 activity (43). Based on this, it may be speculated that, in murine pancreatic cancers, Hilpda is involved in the growth of LDs rather than their shrinkage. The precise mechanism for Hilpda-dependent lipid deposition may depend on the balance of fatty acid uptake, triglyceride biosynthesis and hydrolysis in different cell types and the presence of interacting partners and/or of signals that direct Hilpda's localization in specific subcellular compartments or LD subpopulations.

Acknowledgements

We would like to thank Erich Auer for technical assistance during the early stages of the study.

Funding

This study was in part supported by NCI awards CA191653 (I.P.) and CA197713 (A.J.G.). The OSUCCC shared resources are supported by Cancer Center Support Grant CA016058. NIH had no role in the study design, data generation, the writing of this report or the decision to submit it for publication.

Availability of data and materials

The datasets used and/or analyzed during the current study are available from the corresponding author on reasonable request.

Authors' contributions

JJG and MK contributed to data acquisition and analysis. AJG contributed to study design and funding. NCD substantially contributed to the study design. IP contributed to study design, data analysis, funding, manuscript preparation. All authors read and approved the final manuscript.

Ethics approval and consent to participate

All animal experiments were approved by the Ohio State University's Institutional Animal Care and Use Committee.

Patient consent for publication

Not applicable.

Competing interests

The authors declare that they have no competing interests.

References

1. Hanahan D and Weinberg RA: Hallmarks of cancer: The next generation. Cell 144: 646-674, 2011.
2. Koong AC, Mehta VK, Le QT, Fisher GA, Terris DJ, Brown JM, Bastidas AJ and Vierra M: Pancreatic tumors show high levels of hypoxia. Int J Radiat Oncol Biol Phys 48: 919-922, 2000.
3. Stromnes IM, Hulbert A, Pierce RH, Greenberg PD and Hingorani SR: T-cell localization, activation, and clonal expansion in human pancreatic ductal adenocarcinoma. Cancer Immunol Res 5: 978-991, 2017.
4. Biankin AV, Waddell N, Kassahn KS, Gingras MC, Muthuswamy LB, Johns AL, Miller DK, Wilson PJ, Patch AM, Wu J, *et al*: Pancreatic cancer genomes reveal aberrations in axon guidance pathway genes. Nature 491: 399-405, 2012.
5. Ying H, Kimmelman AC, Lyssiotis CA, Hua S, Chu GC, Fletcher-Sananikone E, Locasale JW, Son J, Zhang H, Coloff JL, *et al*: Oncogenic kras maintains pancreatic tumors through regulation of anabolic glucose metabolism. Cell 149: 656-670, 2012.
6. Commisso C, Davidson SM, Soydaner-Azeloglu RG, Parker SJ, Kamphorst JJ, Hackett S, Grabocka E, Nofal M, Drebin JA, Thompson CB, *et al*: Macropinocytosis of protein is an amino acid supply route in Ras-transformed cells. Nature 497: 633-637, 2013.
7. Kamphorst JJ, Nofal M, Commisso C, Hackett SR, Lu W, Grabocka E, Vander Heiden MG, Miller G, Drebin JA, Bar-Sagi D, *et al*: Human pancreatic cancer tumors are nutrient poor and tumor cells actively scavenge extracellular protein. Cancer Res 75: 544-553, 2015.
8. Palm W, Park Y, Wright K, Pavlova NN, Tuveson DA and Thompson CB: The utilization of extracellular proteins as nutrients is suppressed by mTORC1. Cell 162: 259-270, 2015.
9. Kamphorst JJ, Cross JR, Fan J, de Stanchina E, Mathew R, White EP, Thompson CB and Rabinowitz JD: Hypoxic and Ras-transformed cells support growth by scavenging unsaturated fatty acids from lysophospholipids. Proc Natl Acad Sci USA 110: 8882-8887, 2013.
10. Ma X, Zhao X, Ouyang H, Sun F, Zhang H, Zhou C and Shen H: The metabolic features of normal pancreas and pancreatic adenocarcinoma: Preliminary result of in vivo proton magnetic resonance spectroscopy at 3.0 T. J Comput Assist Tomogr 35: 539-544, 2011.
11. Yabushita S, Fukamachi K, Tanaka H, Fukuda T, Sumida K, Deguchi Y, Mikata K, Nishioka K, Kawamura S, Uwagawa S, *et al*: Metabolomic and transcriptomic profiling of human K-ras oncogene transgenic rats with pancreatic ductal adenocarcinomas. Carcinogenesis 34: 1251-1259, 2013.
12. Zhang G, He P, Tan H, Budhu A, Gaedcke J, Ghadimi BM, Ried T, Yfantis HG, Lee DH, Maitra A, *et al*: Integration of metabolomics and transcriptomics revealed a fatty acid network exerting growth inhibitory effects in human pancreatic cancer. Clinical Cancer Res 19: 4983-4993, 2013.
13. Guillaumond F, Bidaut G, Ouaissi M, Servais S, Gouirand V, Olivares O, Lac S, Borge L, Roques J, Gayet O, *et al*: Cholesterol uptake disruption, in association with chemotherapy, is a promising combined metabolic therapy for pancreatic adenocarcinoma. Proc Natl Acad Sci USA 112: 2473-2478, 2015.
14. Gaglio D, Metallo CM, Gameiro PA, Hiller K, Danna LS, Balestrieri C, Alberghina L, Stephanopoulos G and Chiaradonna F: Oncogenic K-Ras decouples glucose and glutamine metabolism to support cancer cell growth. Mol Syst Biol 7: 523, 2011.

15. Goodman JM: The gregarious lipid droplet. J Biol Chem 283: 28005-28009, 2008.
16. Denko N, Schindler C, Koong A, Laderoute K, Green C and Giaccia A: Epigenetic regulation of gene expression in cervical cancer cells by the tumor microenvironment. Clin Cancer Res 6: 480-487, 2000.
17. Gimm T, Wiese M, Teschemacher B, Deggerich A, Schodel J, Knaup KX, Hackenbeck T, Hellerbrand C, Amann K, Wiesener MS, *et al*: Hypoxia-inducible protein 2 is a novel lipid droplet protein and a specific target gene of hypoxia-inducible factor-1. FASEB J 24: 4443-4458, 2010.
18. Mattijssen F, Georgiadi A, Andasarie T, Szalowska E, Zota A, Krones-Herzig A, Heier C, Ratman D, De Bosscher K, Qi L, *et al*: Hypoxia-inducible lipid droplet-associated (HILPDA) is a novel peroxisome proliferator-activated receptor (PPAR) target involved in hepatic triglyceride secretion. J Biol Chem 289: 19279-19293, 2014.
19. DiStefano MT, Danai LV, Roth Flach RJ, Chawla A, Pedersen DJ, Guilherme A and Czech MP: The lipid droplet protein hypoxia-inducible gene 2 promotes hepatic triglyceride deposition by inhibiting lipolysis. J Biol Chem 290: 15175-15184, 2015.
20. Maier A, Wu H, Cordasic N, Oefner P, Dietel B, Thiele C, Weidemann A, Eckardt KU and Warnecke C: Hypoxia-inducible protein 2 Hig2/Hilpda mediates neutral lipid accumulation in macrophages and contributes to atherosclerosis in apolipoprotein E-deficient mice. FASEB J 31: 4971-4984, 2017.
21. VandeKopple MJ, Wu J, Baer LA, Bal NC, Maurya SK, Kalyanasundaram A, Periasamy M, Stanford KI, Giaccia AJ, Denko NC and Papandreou I: Stress-responsive HILPDA is necessary for thermoregulation during fasting. J Endocrinol 235: 27-38, 2017.
22. DiStefano MT, Roth Flach RJ, Senol-Cosar O, Danai LV, Virbasius JV, Nicoloro SM, Straubhaar J, Dagdeviren S, Wabitsch M, Gupta OT, *et al*: Adipocyte-specific Hypoxia-inducible gene 2 promotes fat deposition and diet-induced insulin resistance. Mol Metab 5: 1149-1161, 2016.
23. Dijk W, Mattijssen F, de la Rosa Rodriguez M, Loza Valdes A, Loft A, Mandrup S, Kalkhoven E, Qi L, Borst JW and Kersten S: Hypoxia-inducible lipid droplet-associated is not a direct physiological regulator of lipolysis in adipose tissue. Endocrinology 158: 1231-1251, 2017.
24. Zhang X, Saarinen AM, Hitosugi T, Wang Z, Wang L, Ho TH and Liu J: Inhibition of intracellular lipolysis promotes human cancer cell adaptation to hypoxia. Elife 6: e31132, 2017.
25. Padmanabha Das KM, Wechselberger L, Liziczai M, De la Rosa Rodriguez M, Grabner GF, Heier C, Viertlmayr R, Radler C, Lichtenegger J, Zimmermann R, *et al*: Hypoxia-inducible lipid droplet-associated protein inhibits adipose triglyceride lipase. J Lipid Res 59: 531-541, 2018.
26. VandeKopple MJ, Wu J, Auer EN, Giaccia AJ, Denko NC and Papandreou I: HILPDA regulates lipid metabolism, lipid droplet abundance, and response to microenvironmental stress in solid tumors. Mol Cancer Res 17: 2089-2101, 2019.
27. Hingorani SR, Wang L, Multani AS, Combs C, Deramaudt TB, Hruban RH, Rustgi AK, Chang S and Tuveson DA: Trp53R172H and KrasG12D cooperate to promote chromosomal instability and widely metastatic pancreatic ductal adenocarcinoma in mice. Cancer Cell 7: 469-483, 2005.
28. Khor VK, Ahrends R, Lin Y, Shen WJ, Adams CM, Roseman AN, Cortez Y, Teruel MN, Azhar S and Kraemer FB: The proteome of cholesteryl-ester-enriched versus triacylglycerol-enriched lipid droplets. PLoS One 9: e105047, 2014.
29. Bian Y, Yu Y, Wang S and Li L: Up-regulation of fatty acid synthase induced by EGFR/ERK activation promotes tumor growth in pancreatic cancer. Biochem Biophys Res Commun 463: 612-617, 2015.
30. Singh A, Ruiz C, Bhalla K, Haley JA, Li QK, Acquaah-Mensah G, Montal E, Sudini KR, Skoulidis F, Wistuba II, *et al*: De novo lipogenesis represents a therapeutic target in mutant Kras non-small cell lung cancer. FASEB J 32: fj201800204, 2018.
31. Qiao S, Koh SB, Vivekanandan V, Salunke D, Patra KC, Zaganjor E, Ross K, Mizukami Y, Jeanfavre S, Chen A, *et al*: REDD1 loss reprograms lipid metabolism to drive progression of RAS mutant tumors. Genes Dev 34: 751-766, 2020.
32. Downes DP, Daurio NA, McLaren DG, Carrington P, Previs SF and Williams KB: Impact of extracellular fatty acids and oxygen tension on lipid synthesis and assembly in pancreatic cancer cells. ACS Chem Biol 15: 1892-1900, 2020.
33. Bensaad K, Favaro E, Lewis CA, Peck B, Lord S, Collins JM, Pinnick KE, Wigfield S, Buffa FM, Li JL, *et al*: Fatty acid uptake and lipid storage induced by HIF-1α contribute to cell growth and survival after hypoxia-reoxygenation. Cell Rep 9: 349-365, 2014.
34. Qiu B, Ackerman D, Sanchez DJ, Li B, Ochocki JD, Grazioli A, Bobrovnikova-Marjon E, Diehl JA, Keith B and Simon MC: HIF2α-dependent lipid storage promotes endoplasmic reticulum homeostasis in clear-cell renal cell carcinoma. Cancer Discov 5: 652-667, 2015.
35. Ackerman D, Tumanov S, Qiu B, Michalopoulou E, Spata M, Azzam A, Xie H, Simon MC and Kamphorst JJ: Triglycerides promote lipid homeostasis during hypoxic stress by balancing fatty acid saturation. Cell Rep 24: 2596-2605.e5, 2018.
36. Rambold AS, Cohen S and Lippincott-Schwartz J: Fatty acid trafficking in starved cells: Regulation by lipid droplet lipolysis, autophagy, and mitochondrial fusion dynamics. Dev Cell 32: 678-692, 2015.
37. Nguyen TB, Louie SM, Daniele JR, Tran Q, Dillin A, Zoncu R, Nomura DK and Olzmann JA: DGAT1-dependent lipid droplet biogenesis protects mitochondrial function during starvation-induced autophagy. Dev Cell 42: 9-21.e5, 2017.
38. Herms A, Bosch M, Reddy BJ, Schieber NL, Fajardo A, Ruperéz C, Fernández-Vidal A, Ferguson C, Rentero C, Tebar F, *et al*: AMPK activation promotes lipid droplet dispersion on detyrosinated microtubules to increase mitochondrial fatty acid oxidation. Nat Commun 6: 7176, 2015.
39. Listenberger LL, Han X, Lewis SE, Cases S, Farese RV Jr, Ory DS and Schaffer JE: Triglyceride accumulation protects against fatty acid-induced lipotoxicity. Proc Natl Acad Sci USA 100: 3077-3082, 2003.
40. Senkal CE, Salama MF, Snider AJ, Allopenna JJ, Rana NA, Koller A, Hannun YA and Obeid LM: Ceramide is metabolized to acylceramide and stored in lipid droplets. Cell Metab 25: 686-697, 2017.
41. de la Rosa Rodriguez MA and Kersten S: Regulation of lipid droplet homeostasis by hypoxia inducible lipid droplet associated HILPDA. Biochim Biophys Acta Mol Cell Biol Lipids 1865: 158738, 2020.
42. Kim SH, Wang D, Park YY, Katoh H, Margalit O, Sheffer M, Wu H, Holla VR, Lee JS and DuBois RN: HIG2 promotes colorectal cancer progression via hypoxia-dependent and independent pathways. Cancer Lett 341: 159-165, 2013.
43. de la Rosa Rodriguez MA, Gemmink A, van Weeghel M, Aoun ML, Singh R, Borst JW and Kersten S: Hypoxia-inducible lipid droplet-associated interacts with DGAT1 to promote lipid storage in hepatocytes. bioRxiv: Feb 27, 2020 (Epub ahead of print). doi: org/10.1101/2020.02.26.966374.